

Radiation Effects on Spacecraft & Aircraft

Clive Dyer⁽¹⁾

⁽¹⁾ Space Department, QinetiQ, Cody Technology Park, Farnborough, Hampshire GU14 0LX, UK,
Email: csdyer@space.QinetiQ.com

ABSTRACT

Satellite systems are vulnerable to Space Weather through its influence on energetic charged particle and plasma populations, which produce a variety of effects, including total dose, lattice displacement damage, single event effects (SEE), noise in sensors and electrostatic charging. In addition aircraft electronics and aircrew are subjected to atmospheric secondary radiation produced by cosmic rays and solar particle events. European Union legislation requires the control of aircrew exposure, while the decreasing feature size of modern microelectronics is leading to increased vulnerability to SEE. Such effects are also starting to afflict sea-level systems. Examples of all the above effects are given from observed spacecraft anomalies or on-board dosimetry. These demonstrate the need for improved monitoring, understanding and prediction accuracy for Space Weather.

1. SPACE RADIATION ENVIRONMENT

1.1 Cosmic Rays

These comprise 85% protons, 14 % alpha particles, and 1% heavier ions covering the full range of elements, some of the more abundant being, for example, carbon and iron nuclei. They are partly kept out by the earth's magnetic field and have easier access at the poles compared with the equator. From the point of view of space systems it is particles in the energy range 1-20 GeV per nucleon which have most influence. An important quantity is the rigidity of a cosmic ray which measures its resistance to bending in a magnetic field and is defined as the momentum-to-charge ratio for which typical units are GV. At each point on the earth it is possible to define a threshold rigidity or cut-off which a particle must exceed to be able to arrive there. Values vary from 0 at the poles to about 17 GV at the equator. The influence of Space Weather is to provide a modulation in antiphase with the sunspot cycle and with a phase lag which is dependent on energy.

1.2 Radiation Belts

These divide into two belts, an inner belt extending to 2.5 earth radii and comprising energetic protons up to 600

MeV together with electrons up to several MeV, and an outer belt comprising mainly electrons extending to 10 earth radii. The slot region between the belts has lower intensities but may be greatly enhanced for up to a year following one or two solar events in each solar cycle. The outer belt is highly dynamic and is driven by solar wind conditions. These variations are examples of Space Weather. Standard models of the radiation belts are AP8 for protons and AE8 for electrons [1,2] but these take little account of Space Weather variations apart from having different versions for solar maximum and minimum. The earth's atmosphere removes particles from the radiation belts and low earth orbits can be largely free of trapped particles. However because of the displacement of the dipole term in the geomagnetic field away from the earth's centre, there is a region in the South Atlantic where the trapped radiation is found at lower altitudes. This is called the South Atlantic or Brazilian Anomaly (SAA) and dominates the radiation received by low earth orbits. In addition, highly inclined low earth orbits intersect the outer belt electrons at high latitudes in the so-called horn regions. An artist's impression of the radiation belts is given in Fig. 1, which shows how a high inclination orbit intersects the outer belt. As illustrated in section 3, Space Weather influences the upper atmosphere leading to variations in the particle population in the SAA.

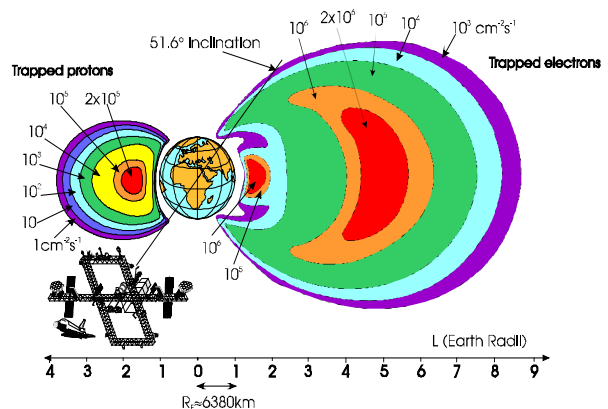


Fig. 1. Artist's impression of the radiation belts.

1.3 Solar Particles

In the years around solar maximum the sun is an additional sporadic source of lower energy particles accelerated during certain solar flares and in the

subsequent coronal mass ejections. These solar particle events last for several days at a time and comprise both protons and heavier ions with variable composition from event to event. Energies typically range up to several hundred MeV and have most influence on high inclination or high altitude systems. Occasional events produce particles of several GeV in energy and these can reach equatorial latitudes.

1.4 Atmospheric Secondaries

The primary cosmic rays interact with air nuclei to generate a cascade of secondary particles comprising protons, neutrons, mesons, electrons, photons and nuclear fragments. The intensity of radiation builds up to a maximum at 60000 feet (the Pfozter maximum) and then slowly drops off to sea level. At normal aircraft cruising altitudes the radiation is several hundred times the ground level intensity and at 60000 feet a factor three higher again. Solar particles are less penetrating and only a few events in each cycle can reach aircraft altitudes or ground level.

2. RADIATION EFFECTS

2.1 Total Dose Effects

Dose is used to quantify the effects of charge liberation by ionisation and is defined as the energy deposited as ionisation and excitation per unit mass of material (note that the material should be specified). SI units are J/kg or grays (= 100 rads, where 1 rad is 100 ergs/g). The majority of effects depend on rate of delivery and so dose-rate information is required. Accumulated dose leads to threshold voltage shifts in CMOS devices due to trapped holes in the oxide and the formation of interface states. In addition increased leakage currents and gain degradation in bipolar devices can occur.

2.2 Displacement Damage

A proportion of the energy-loss of energetic radiation goes into lattice displacement damage and it is found that many effects scale with NIEL, defined as the non-ionising energy loss per unit mass. Examples of damage effects are reduction in bipolar transistor gain, reduced efficiencies in solar cells, light emitting diodes and photodetectors, charge transfer inefficiency in charge coupled devices and resolution degradation in solid-state detectors.

2.3 Single Event Effects

For cosmic rays the density of charge deposition by ionisation is proportional to the square of the atomic number so that the heavier species can deposit enough charge in a small volume of silicon to change the state of a memory cell, a one becoming a zero and vice versa.

Thus memories can become corrupted and this could lead to erroneous commands. Such soft errors are referred to as single event upsets (SEU). Sometimes a single particle can upset more than one bit to give what are called multiple bit upsets (MBU). Certain devices could be triggered into a state of high current drain, leading to burn-out and hardware failure; such effects are termed single event latch-up or single event burn-out. In other devices localised dielectric breakdown and rupture can occur (single event gate rupture and single event dielectric failure). These deleterious interactions of individual particles are referred to as single event effects (SEE). For space systems SEEs have become increasingly important over the last fifteen years and are likely to become the major radiation effects problem of the future. For avionics SEEs are the main radiation concern but total dose can be of significance for aircrew (although the latter is in fact an accumulation of SEE in tissue).

The severity of an environment is usually expressed as an integral linear energy transfer spectrum which gives the flux of particles depositing more than certain amount of energy (and hence charge) per unit pathlength of material. Energy deposited per unit pathlength is referred to as linear energy transfer (LET) and the common units are MeV per g cm⁻² or per mg cm⁻². Devices are characterised in terms of a cross-section (effective area presented to the beam for a SEE to occur) which is a function of LET. For each device there is a threshold LET below which SEE does not occur. As device sizes shrink these thresholds are moving to lower LET and rates are increasing. In addition to directly ionising interactions with electrons, particles may interact with atomic nuclei thus imparting a certain recoil energy and generating secondary particles. Both the recoiling nucleus and secondary charged particles are highly ionising so that if such a reaction occurs in, or adjacent to, a device depletion region a SEE may result. Collisions with nuclei are less probable than collisions with orbital electrons but when certain particle fluxes are high this mechanism can dominate. This occurs in the earth's inner radiation belt where there are intense fluxes of energetic protons. It can also occur in the atmosphere where there is a build-up of significant fluxes of secondary neutrons. This mechanism is thought to be the dominant SEE hazard for current and near future avionics at most altitudes.

For radiation effects on biological systems it is found that there is a strong dependence on LET and so dose equivalents are used. Quality factors are defined to measure the enhancement in the effect compared with lightly ionising electrons or photons. These factors can be as large as 20 for heavy ions and fast neutrons. The product of dose and quality factor gives the dose equivalent, for which the

SI units are sieverts (the dose equivalent of the rad is the rem, so that 1 sievert = 100 rem).

2.4 Background Noise in Sensors

Spurious counts are produced in many detector systems and these depend on the size distribution of individual depositions and can occur from both prompt ionisation and delayed depositions due to induced radioactivity

2.5 Electrostatic Charging

Surface charging can occur when spacecraft are bathed in energetic plasmas (several keV electron temperature) without the presence of neutralising cold plasma. This can occur in the geomagnetic tail region during geomagnetic storms and the subsequent discharges can couple into spacecraft systems. Internal charging, or deep dielectric charging as it is commonly called, can occur during energetic (several MeV) electron enhancements. Electrons penetrating the thin skin can be trapped in dielectric materials near the surface and sufficient build-up can occur over a few days to result in a damaging electron caused electromagnetic pulse (ECEMP).

3. EXAMPLES OF EFFECTS

3.1 Total Dose

It is difficult to obtain hard evidence of failures as there are usually insufficient diagnostics and effects are readily confused with ageing. Exceptions are when deliberate experiments are performed, such as on the Combined Release and Radiation Effects Spacecraft (CRRES) or the current Microelectronics and Photonics Test Bed (MPTB). Sensitive pMOS transistors are frequently used as RADFETs to deliberately monitor the accumulated dose via the measured threshold voltage shift. On MPTB leakage currents in 16-Mbit DRAMs were seen to increase rapidly leading to non-functionality in October 1998 following an extended period of high dose rates as measured by adjacent RADFETs. This period followed the solar particle event of 24 August 1998 where the ensuing geomagnetic disturbance led to enhanced electron fluxes in the outer radiation belt [3,4].

3.2 Displacement Damage

The clearest examples arise from observations of degradations in solar-array efficiency where sharp drops can occur during solar particle events. For example, drops in efficiency of 4% in GEO [5] and 2% in LEO [6] were observed during the large solar particle events of September and October 1989. The March 1991 event was responsible for removing the equivalent of 3 years lifetime from the GOES spacecraft [7]. More recently the solar proton event of 14 July

2000 led to a 2% drop in solar array efficiency for the SOHO spacecraft in interplanetary space.

Optocoupler degradation under proton irradiation is far greater than when irradiated by gamma rays or electrons due to displacement damage in both the light-emitting diode and photodetector elements [8]. Recently optocoupler failures have been observed on the TOPEX spacecraft due to reduced current transfer efficiency resulting from proton damage. Such failures will be susceptible to Space Weather through variations in the inner belt protons and solar protons.

Charge-coupled devices show reduction in charge-transfer efficiency under proton irradiation and the CHANDRA X-ray astronomy mission has been severely afflicted by low energy protons scattering onto the CCDs. While protective measures in the XMM mission have limited the damage, the charge transfer efficiency shows significant changes with solar particle events, particularly that of 14 July 2000 [9].

3.3 Single Event Effects

A classic example of cosmic-ray induced upsets was experienced by the NASA/DoD Tracking and Data Relay Satellite (TDRS-1) which incorporated sensitive RAM chips in the Attitude Control System. Rates of 1 to 2 per day clearly showed modulation with cosmic rays, while during the solar particle events of September to October 1989 rates reached 20 per day [10]. As a result expensive ground control procedures had to be employed on what was intended to be an autonomous spacecraft.

A classic example of hardware failure occurred in the PRARE (Precision Ranging Experiment) instrument carried on the ERS-1 (European Remote Sensing Spacecraft). A latch-up failure occurred in the heart of the SAA after 5 days and led to loss of the instrument. Subsequent analysis and ground testing proved this diagnosis [11].

Commercial, unhardened systems are particularly vulnerable. For example IBM ThinkPad computers on the MIR Space station have shown upsets every nine hours [12], while other laptop computers on Space Shuttle have shown upset rates of one per hour [13].

Examples will be given to show the influence of Space Weather on the SEE environment from sea level to interplanetary space.

3.3.1 Avionics

In the last twelve years it has been realised that single event effects will also be experienced by sensitive electronics in aircraft systems, which are subjected to

increasing levels of cosmic radiation and their secondaries as altitude increases. Significant effort has gone into monitoring the environment and analysing operational systems for SEUs. At the same time increasing concern with respect to dose to aircrew is reflected in an EU directive, effective May 2000, whereby annual doses in excess of 1mSv must be estimated and controlled.

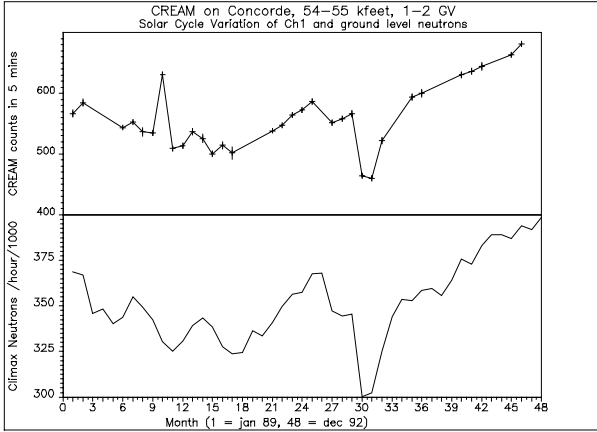


Fig. 2. Monthly mean count rates from CREAM on Concorde from Jan 89 to Dec 92 compared with ground level neutron monitor at Climax.

The CREAM (Cosmic Radiation Effects and Activation Monitor) and CREDO (Cosmic Radiation Effects and Dosimetry) detectors are designed to monitor those aspects of the space radiation environment of concern for electronics; i.e. charge-deposition spectra, linear energy transfer spectra and total dose. In the CREAM and CREDO-I instruments the SEU environment is monitored by means of pulse-height analysis of the charge-deposition spectra in ten pin diodes, each 1 cm² in area and 300 μm in depth. A version of the CREAM detector made regular flights on-board Concorde G-BOAB between November 1988 and December 1992 and results from 412 flights between London and New York or Washington DC are shown in Fig.2 [14]. This shows the count rate in CREAM channel 1 (19fc to 46fc, LET 6.1 MeV cm² g⁻¹) plotted as monthly averages for the ranges 54-55 kfeet and 1-2 GV. The rates show a clear anticorrelation with the solar cycle and track well with the neutron monitor at Climax Colorado (altitude 3.4 km, cut-off rigidity 2.96 GV). The enhanced period during September and October 1989 comprised a number of energetic solar particle events observed by ground level, high latitude neutron monitors and the Concorde observations showed instantaneous increases of up to a factor 10 and flight-averaged increases of up to a factor 6 [15,16].

An increasing body of data on upsets in avionics systems is being accumulated. A commercial computer was temporarily withdrawn from service when bit-errors were found to accumulate in 256-Kbit CMOS

SRAMs [17]. Following ground irradiations by neutrons, the observed upset rate of 4.8×10^{-8} upsets per bit-day at conventional altitudes (35000 feet) was found to be explicable in terms of SEUs induced by atmospheric neutrons. In an investigation of single event upsets in avionics, Taber and Normand [18] have flown a large quantity of CMOS SRAM devices at conventional altitudes on a Boeing E-3/AWACS aircraft and at high altitudes (65000 feet) on a NASA ER-2 aircraft. Upset rates in the IMS1601 64Kx1 SRAM varied between 1.2×10^{-7} per bit-day at 30000 feet and 40° latitude to 5.4×10^{-7} at high altitudes and latitudes. Reasonable agreement was obtained with predictions based on neutron fluxes. Recently upset rates of around 1 per 200 hours in the Boeing 777 autopilot have been shown to fit predictions based on atmospheric neutron fluxes [19].

Recently calculations have been performed on the enhanced environments due to the large solar particle events of 23 February 1956 and 29 September 1989 [20]. Figs. 4 and 5 show the calculated neutron flux variations with altitude and rigidity cut-off compared with quiet-time cosmic rays. The solar particle enhancements have a very steep dependence on altitude and cut-off rigidity. Increases with respect to cosmic rays at high latitude and altitude (17 km) are a factor 330 for September 1989 and 1000 for February 1956. Even for the September 1989 event, flight doses of several mSv are possible for near polar routes at conventional altitudes, while upset rates in a Gbyte of modern SRAM memory would be around one per minute.

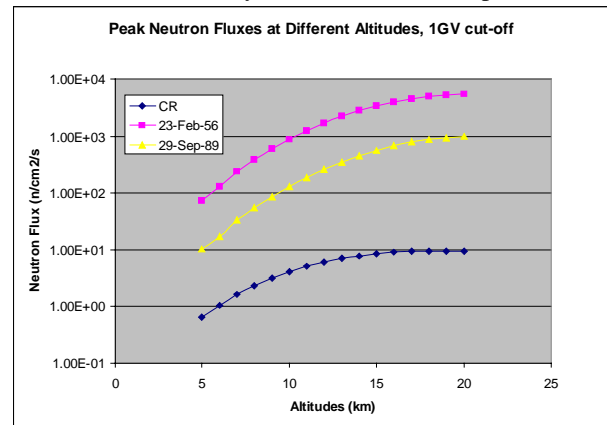


Fig.3. The calculated altitude profiles of the peak neutron fluxes at 1 GV show large increases for the solar particle events of 23 Feb 1956 and 29 September 1989 compared with cosmic ray fluxes. The solar particle fluxes also increase much more rapidly with altitude.

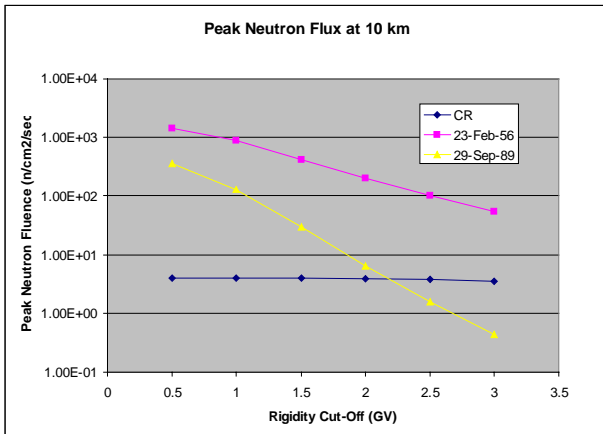


Fig.4. Calculated peak neutron fluxes for the solar particle events at 10 km show a very steep dependence on cut-off rigidity over the range 0.5 to 3 GV while the cosmic ray levels are very flat.

3.3.2 Shuttle

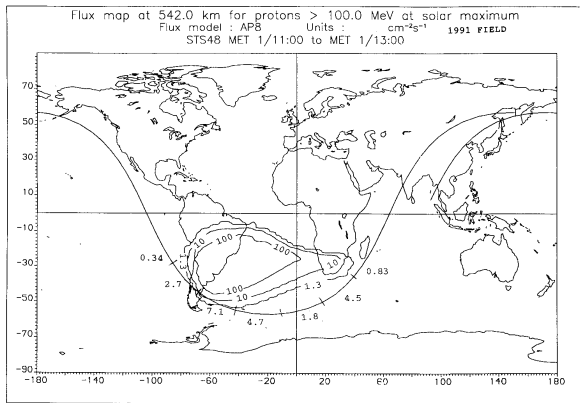


Fig. 5. Ground track of orbit 23 for STS-48 is shown with respect to proton flux contours ($E > 100$ MeV) from AP-8 & 1991 field. With the updated field the orbit intersects the SAA. An additional peak is seen off of South Africa due to the new radiation belt created in March 1991.

The CREAM detector has flown on a number of Shuttle missions between 1991 and 1998. Results show the movement of the SAA region [21] and also intersection of the new radiation belt formed in March 1991. This is illustrated in Fig. 5 where the ground track of orbit 23 for STS-48 is shown with respect to the SAA contours obtained using the 1991 field. It can be seen that the orbit just clips the contours to the Southwest and would miss for 1970 field contours. For this orbit there is a second peak observed off of South Africa which is not predicted by either field model. This region is where the $L=2.5$ shell intersects this altitude orbit and the high fluxes are due to the second proton belt observed by CRRES to be created by the solar flare event of 23 March 1991.

3.3.3 UoSAT Series

UOSAT-2 was launched in 1984 into a 700 km, near polar, sun-synchronous orbit. Following the realisation of the significance of the data the SEUs have been logged to within 8.25 minutes accuracy since 1988. Data have been presented in [22] from which Fig. 6 shows that the majority of events occur in the SAA region, while a further contribution from cosmic rays is seen to cluster at high latitudes. In addition the flare event of October 1989 gave a large increase in upsets.

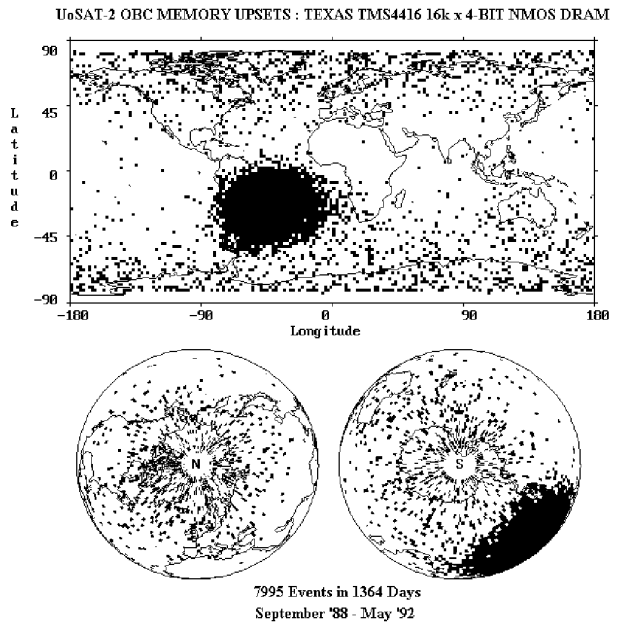


Fig. 6. Geographical distribution of SEUs in nMOS DRAMs on UoSAT-2 showing clustering of proton events in the SAA and cosmic-ray events at high latitude.

The interest in such SEU data led us to develop the CREAM instrument developed for Concorde and Shuttle into the CREDO instrument for free-flyers and this was first launched on UoSAT-3 into 800km, 98.7° orbit in January 1990. Continuous data on both environment and upsets have been obtained since April 1990 until October 1996, covering conditions ranging from solar maximum to minimum and including a large number of solar flare events, the most notable of which was the March 1991 event responsible for creating the new proton belt as observed by CRRES, Shuttle and UoSAT-3 itself.

The SAA proton fluxes have evolved over this time and actually fell during the first 2 years reaching a broad minimum in 1992 before steadily increasing by 34% [23]. This is due to decreased atmospheric losses as the upper atmosphere contracts towards solar minimum but there is an obvious phase lag due to the removal time. Contour plots obtained in 1992 and 1995 are compared in Fig. 7 and show both a general increase in intensity,

as discussed above, and a north-westward drift due to the evolution of the geomagnetic field.

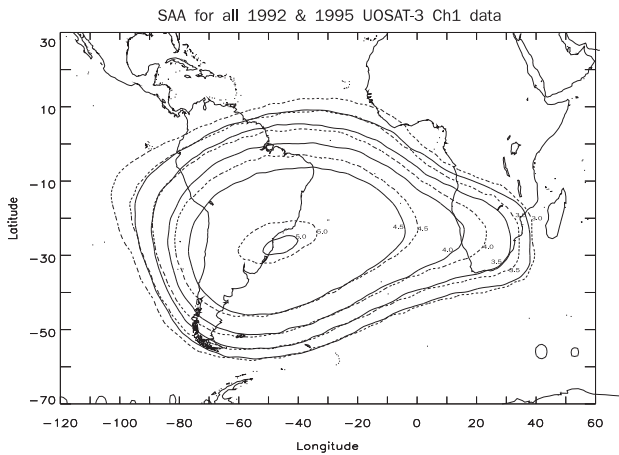


Fig. 7. Contour plots from channel 1 of CREDO on UoSAT-3 show both an increase and a north-westward drift in the SAA between 1992 (solid lines) and 1995 (dotted lines).

3.3.4 CRRES

The Combined Release and Radiation Effects Spacecraft (CRRES) was the most comprehensively instrumented spacecraft ever launched with the purpose of performing collateral measurements of the radiation environment and its effects on a wide range of state-of-the art and future electronics technologies. The two-ton spacecraft was launched into a geostationary transfer orbit (350 x 33500 km, 18.1° inclination) on 25 July 1990 and operated until October 1991. In March 1991 CRRES observed a solar-particle event and geomagnetic storm responsible for the creation of a new radiation belt of both energetic protons [24] and very energetic electrons [25] at around L=2.5. Large increases in both dose-rates [26] and SEU rates were observed following this event. Figs. 8 and 9, taken from [24] show the changed profile in upsets around the orbit following this event. The influence of the second proton belt can be clearly seen.

3.3.5 MPTB

The Microelectronics and Photonics test bed comprises 23 boards of test electronics and a CREDO-3 radiation environment monitor board and was launched into highly eccentric orbit in November 1997[3,4]. In Fig. 10, the proton monitor shows the increasing solar modulation of cosmic rays as well as a number of significant solar particle events. Of these the "Bastille Day" event of 14 July 2000 is by far the most intense, rivalling the October 1989 event. Test boards of 16-Mbit DRAMs showed large numbers of SEUs which correlated with the particle fluxes as measured by CREDO-3. This is illustrated in Fig. 11 The spikes seen before and after the event are passages through the inner radiation belt.

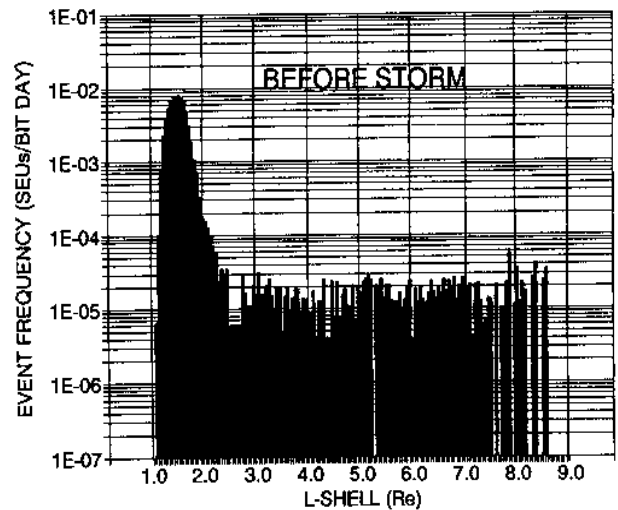


Fig. 8. SEU frequency for 35 proton-sensitive devices for the first 585 orbits (25 July 1990 to 22 March 1991) of CRRES are shown as a function of L-shell. The peak at L=1.5 coincides with the heart of the inner radiation belt [24].

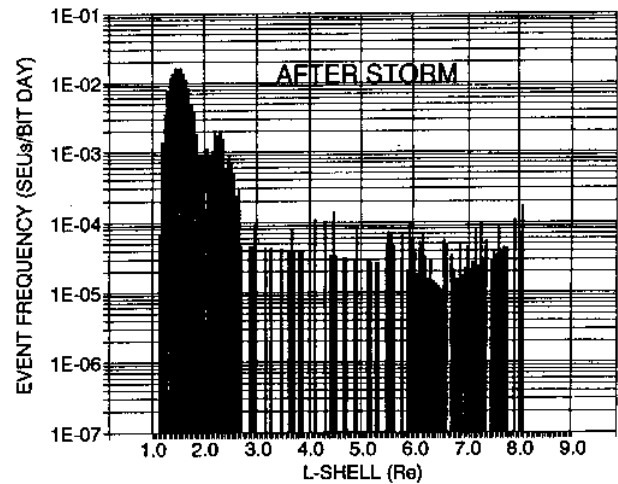


Fig. 9. As above but for the 141 orbits following the solar-proton event of 23-29 March 1991. The creation of a second proton belt leads to a peak at L=2.3 to 2.5

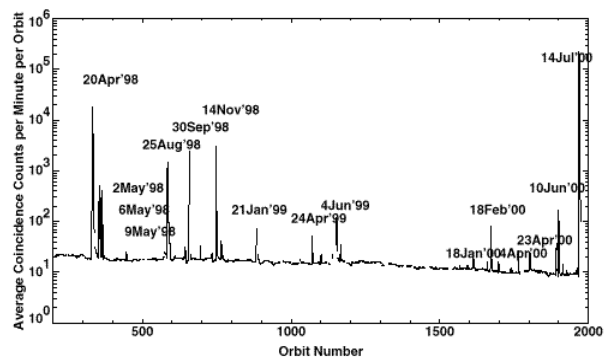


Fig. 10. Orbit-averaged proton fluxes with inner-belt passes removed showing cosmic-ray modulation by a factor two and a number of solar particle events, including the large event on 14 July 2000.

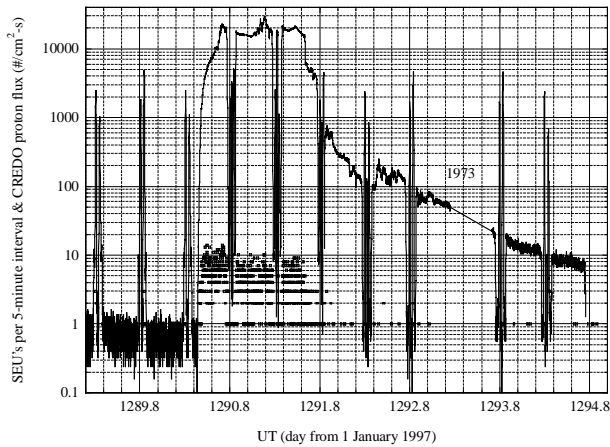


Fig. 11: Proton flux from the CREDO instrument versus UT for the period just before, during and after the Bastille-day event (12-23 July 2000, orbits 1964 through 1975 with orbit 1973 missing) along with upsets per 5-minute interval in the two MPTB boards A6 & B6. The curve is the CREDO flux and the individual data points (squares) represent the individual SEUs. Data is missing for orbit 1973 as indicated in the figure.

The CREDO-3 instrument measured the integral LET spectrum during the event and this is compared with the preceding quiet-time spectrum and the CREME96 model worst-case flare spectrum in Fig.12. The latter is based on the October 1989 event and it can be seen that the July 2000 event matches this at low LET (i.e. protons) but is less intense at higher LET so that less heavy ions were present. Use of this measurement shows that the SEUs were approximately 50% due to heavy ions and 50% due to proton interactions [27].

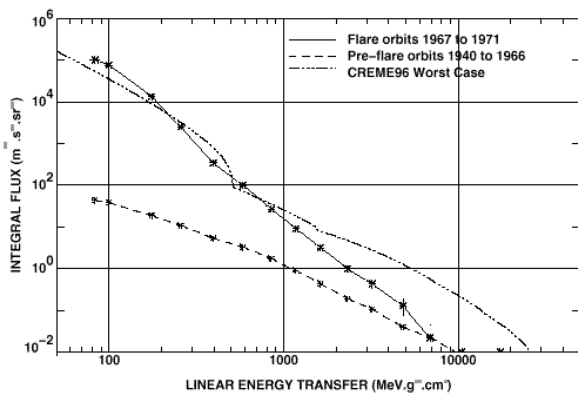


Fig. 12. Integral LET spectra averaged over the 5 peak orbits of the event of 14 July 2000 are compared with spectra from the preceding quiet-time period and the CREME96 worst week model.

3.4 Background Noise in Sensors

Enhanced background rates in SOHO and IRAS detectors due to cosmic rays, spacecraft secondaries and solar particle events are discussed elsewhere in these proceedings. Gamma-ray and X- ray detectors are

particularly sensitive to background including delayed events from induced radioactivity [28,29].

3.5 Spacecraft Charging

Numerous anomalies have occurred from both surface and deep dielectric charging. Some of these have proved fatal (e.g. ANIK E1), while the more numerous, non-fatal anomalies enable the variations with Space Weather to be seen. The environmental parameters influencing charging have been reviewed in [30] from which the following figures are taken.

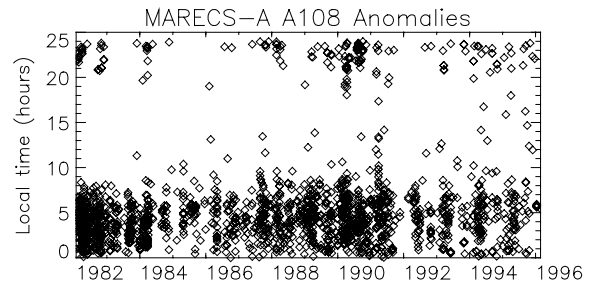


Fig.13. MARECS-A Anomalies vs year and local time

MARECS-A is a classic case of surface charging, as illustrated in Fig.13, where anomalies can be seen to cluster during midnight to 0600 local time due to the eastwards drift of the enhanced electrons in the magnetotail during geomagnetic substorms. Enhanced rates around solar maximum are also seen.

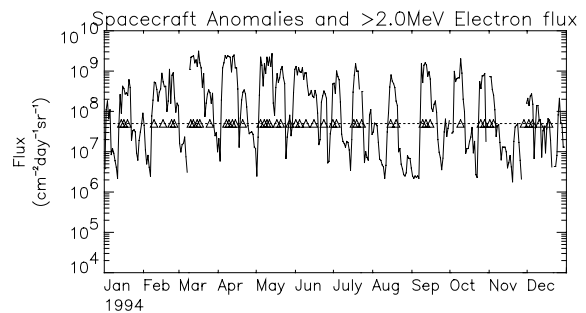


Figure 14. DRA-δ anomalies (Δ) & energetic electron fluxes.

DRA-δ anomalies are a classic example of deep dielectric charging and the rates correlate with energetic electron enhancements in the outer radiation belt. Fig.14 illustrates the huge variability in the outer zone and the presence of a 27- day recurrence period from fast solar wind streams. For this phenomenon there is evidence for enhanced rates towards solar minimum.

4. DISCUSSION

Space Weather variability makes predictions of effects difficult while future systems are likely to be more

vulnerable due to use of higher performance digital electronics of increasing sensitivity. In addition there will be a decreasing supply of radhard components which were traditionally made available through military programmes. Vulnerability is extending to aircraft electronics and dose to aircrew must be estimated and controlled. Solar particle events can significantly enhance the environment at aircraft altitudes. There is clearly a strong need for an active programme in Space Weather modelling, monitoring and prediction in order to ensure long-life, cost effective systems in Space and the upper atmosphere.

5. REFERENCES

1. J I Vette, "The NASA/National Space Science Data Center Trapped Radiation Environment Model Program (TREMPE) (1964-1991)," NSSDC/WDC-A-R&S 91-29, NASA/GSFC, Nov 1991.
2. J I Vette, "The AE-8 Trapped Electron Model Environment," NSSDC/WDC-A-R&S 91-24, NASA/GSFC, Nov 1991.
3. C S Dyer, C Sanderson, R Mugford, C Watson, C Peerless, "Radiation environment of the Microelectronics and Photonics Test Bed as measured by CREDO-3," IEEE Trans. Nucl. Sci., Vol. 47, No. 3, pp481-485, June 2000.
4. C S Dyer, P R Truscott, C Sanderson, C Watson, C L Peerless, P Knight, R Mugford, T Cousins, R Noulty, "Radiation environment measurements from CREAM and CREDO during the approach to solar maximum," IEEE Trans. Nucl. Sci., Vol. 47, No. 6, pp2208-2217, Dec. 2000.
5. L J Goldhammer, "Recent Solar Flare Activity And Its Effects On In-Orbit Solar Arrays," IEEE 21st PVSC, Vol II, 1241-1248, 1990.
6. A Jalinat, G Picart, E Rapp, P Samson, "In-Orbit Behaviour Of SPOT 1,2 and 3 Solar Arrays," ESA SP-416, 627-631, Sept 1998.
7. M A Shea, D F Smart, J H Allen, D C Wilkinson, "Spacecraft Problems in association with episodes of intense solar activity and related terrestrial phenomena during March 1991," IEEE Trans. Nucl. Sci., NS-39, 6, 1754-1760, Dec 1992.
8. B G Rax, C I Lee, A H Johnston, C E Barnes, "Total dose and proton damage in optocouplers," IEEE Trans. Nucl. Sci., NS-43, 6, 3167-3173, Dec 1996.
9. A F Abbey, R M Ambrosi, D R Smith, E Kendziorra, I Hutchinson, A Short, P Bennie, A Holland, T Clauss, M Kuster, W Rochow, M Brandt, M J L Turner, A Wells, "The effect of low energy protons on the operational characteristics of EPIC-MOS CCDs," Proceedings of RADECS2001.
10. D C Wilkinson, S C Daughtridge, J L Stone, H H Sauer, P Darling, "TDRS-1 Single Event Upsets And The Effect Of The Space Environment," IEEE Trans. Nucl. Sci., 38, 6, 1708-1712, Dec 1991.
11. L Adams, E Daly, R Harboe-Sorenson, R Nickson, J Haines, W Shafer, M Conrad, H Greich, J Merkel, T Scwall, R Henneck, "A Verified Proton Induced Latch-Up In Space," IEEE Trans. Nucl. Sci., 39, 6, 1804-1808, Dec. 1992.
12. M Martigno, R Harboe-Sorenson, "IBM ThinkPad Radiation Testing And Recovery During EUROMIR Missions," IEEE Trans. Nucl. Sci., 42, 6, 2004-2009, Dec 1995.
13. A L Klausman, "Effects Of Space Flight On Small Portable Computers," MSc Thesis, University of Houston at Clear Lake, Dec 1995.
14. A Sims, C Dyer, C Peerless, K Johansson, H Pettersson, J Farren, "The single event upset environment for avionics at high latitude", IEEE Trans. on Nuc. Sci., 41, 6, pp 2361-2367, Dec 1994.
15. C S Dyer, A J Sims, J Farren, J Stephen, "Measurements of the SEU environment in the upper atmosphere," IEEE Trans. on Nuc. Sci., NS-36, No 6, pp 2275-2280, Dec. 1989.
16. C S Dyer, A J Sims, J Farren, J Stephen, C Underwood, "Comparative measurements of the single event upset and total dose environments using the CREAM instruments", IEEE Trans. on Nuc. Sci., NS-39, No 3, pps 413-417, June 1992.
17. J Olsen, P E Becher, P B Fynbo, P Raaby, J Schultz, "Neutron Induced Single Event Upsets In Static RAMs Observed at 10 km Flight Altitude," IEEE Trans. Nucl. Sci., 40, 2, 74-77, April 1993.
18. A Taber, E Normand, "Single Event Upset In Avionics," IEEE Trans. Nucl. Sci., 40, 2, 120-125, April 1993.
19. E Normand, "Correlation of inflight neutron dosimeter and SEU measurements with atmospheric neutron model," IEEE Trans. Nucl. Sci., Dec. 2001 (in press).
20. C S Dyer, F Lei, "Monte Carlo calculations of the influence on aircraft radiation environments of structures and solar particle events," IEEE Trans. Nucl. Sci., Dec. 2001 (in press).
21. C S Dyer, P R Truscott, C L Peerless, C J Watson, H E Evans, P Knight, M Cosby, C Underwood, T Cousins, R Noulty, "Updated measurements from CREAM & CREDO & implications for environment and shielding models," IEEE Trans. Nucl. Sci., NS-45, 3, 1584-1588, June 1998.
22. C Underwood, E Daly, R Harboe-Sorensen, "Observation and analysis of single-event upset phenomena on-board the UOSAT-2 Satellite", Proceedings of the ESA Space Environment Workshop, ESTEC, Oct 1990.
23. C I Underwood, M K Oldfield, C S Dyer, A J Sims, " Long-term trend in the LEO radiation environment as measured by radiation monitors on-board three UoSAT-class micro-satellites," ESA SP-392, 37-44, Sept 1996.
24. E Mullen, M Gussenhoven, K Ray, M Violet, "A double-peaked inner radiation belt: cause and effect as seen on CRRES", IEEE Trans. on Nuc. Sci., 38, 6, pp 1713-1717, Dec 1991.
25. J B Blake, M S Gussenhoven, E G Mullen, and R W Fillius, "Identification of an unexpected radiation hazard," IEEE Trans on Nuc Sci, NS-39, No 6, pp 1761-1764, Dec 1992.
26. M Gussenhoven, E Mullen, M Sperry, K Kerns, J Blake, "The effect of the March 1991 storm on accumulated dose for selected satellite orbits: CRRES dose models", IEEE Trans. Nucl. Sci., 39, 6, pp 1765-1772, Dec 1992.
27. A Campbell, S Buchner, E Petersen, B Blake, J Mazur, C Dyer, P Marshall, "SEU measurements and predictions on MPTB for a large energetic solar particle event, Proceedings of RADECS2001.
28. C S Dyer, P R Truscott, H E Evans, N Hammond, C Comber, S Battersby, "Calculations and observations of induced radioactivity in spaceborne materials", IEEE Trans. Nucl. Sci., 41, 3, pp 438-444, June 1994.
29. C S Dyer, P R Truscott, H E Evans, C L Peerless, "Simulation of spacecraft secondary particle emissions & their energy deposition in CCD X-ray detectors," IEEE Trans. Nucl. Sci., NS-43, 6, 2709-2714, Dec 1996.
30. G L Wrenn, R J K Smith, "Probability factors governing ESD effects in geosynchronous orbit," IEEE Trans. Nucl. Sci., NS-43, 6, pp 2783-2789, Dec 1996.